Effect of Antenna Location on GNSS Positioning for ITS Applications

Martti Kirkko-Jaakkola*, Shaojun Feng†, Yanrong Xue†‡, Xin Zhang†, Salomon Honkala*, Stefan Söderholm*, Laura Ruotsalainen*, Washington Ochieng†, and Heidi Kuusniemi*
*Department of Navigation and Positioning, Finnish Geospatial Research Institute FGI, National Land Survey of Finland
02430 Masala, Finland; Email: firstname.lastname@nls.fi
†Centre for Transport Studies, Department of Civil and Environmental Engineering, Imperial College
London SW7 2AZ, United Kingdom
‡National Time Service Center, Chinese Academy of Sciences
Xi'an 710600, China

***Abstract*—The proliferation of GNSS-receiving mobile devices in the consumer market and the growth of the Intelligent Transportation Systems sector have raised a lot of interest in low-cost precise positioning. However, GNSS signal quality is degraded inside the metal body of a vehicle, which is where the antenna of a portable device is to be located. This article investigates the effect of antenna location on precise low-cost GNSS positioning for a road vehicle. We compare a roof-mounted GNSS receiver with an identical receiver having the antenna on the dashboard and a tailored smartphone also located inside the cabin; both the availability of raw carrier phase measurements and the resulting horizontal precise point positioning accuracy are evaluated. The test results show that the 90 % circular error probable is degraded by several meters inside the vehicle. Moreover, most of the evaluated accuracy metrics indicate that the low-cost GNSS receiver with antenna inside the cabin achieved a positioning accuracy at least 50 % better than the smartphone located next to it when using the same satellite systems.**

***Index Terms*—global navigation satellite systems; intelligent transportation systems; mobile devices; precise point positioning**

I. Introduction

Various applications in the field Intelligent Transportation Systems (ITS) need to know the position of the vehicle of interest [1]. The conventional positioning solution is to utilize Global Navigation Satellite Systems (GNSS) which is well known to independently deliver an accuracy in the order of 5 meters in benign reception conditions, i.e., with a sky view unobstructed by tall buildings or other obstacles. While this is adequate for many applications such as route guidance, it is not sufficient for, e.g., collision avoidance or identifying the lane or parking space occupied by the vehicle.

If proper assistance data are available, the accuracy of GNSS can be improved to the sub-meter level; even centimeter precision or better can be achieved with professional multi-frequency equipment [2], [3]. Such high-accuracy positioning has usually been done with expensive dual-frequency receivers, but implementing the same techniques with low-cost single-frequency devices has been an active research topic for more than a decade [4]. Even a sub-meter position accuracy without expensive hardware would be a door opener for several ITS applications.

The increased availability of GNSS-enabled mobile devices on the market is definitely interesting for ITS [5]. However, the smartphone will be located inside the vehicle, most likely in the user's pocket or in a dedicated mount on the dashboard. Therefore, the GNSS reception will be less favorable than for an antenna mounted on the roof of the vehicle. In this paper, we compare a low-cost GNSS receiver connected to a rooftop patch antenna with an identical receiver and a smartphone both mounted inside the vehicle on the dashboard. The goal is to investigate the quality degradation of GNSS measurements made inside the cabin caused by shadowing by the body of the vehicle.

There have been studies on the accuracy of integrated GNSS receivers in smartphones [6], [7], but these have mostly been made using the position solutions output by the phone's operating system or a third-party application. In that approach, there is no knowledge about the sensors and filter models used to produce the position estimate, and the positioning system must be treated as a black box. In this paper, a commercial smartphone model running a custom firmware is used in order to access the raw pseudorange and carrier phase measurements made by the internal GNSS receiver of the smartphone, and these measurements are processed using the same software that is used for the other receivers. It has been shown that precise GNSS positioning is possible using the antenna of a smartphone [8], but it is not straightforward to implement using the actual measurements made by the integrated GNSS chip [9].

This article is organized as follows. First, traditional precise positioning methods are briefly reviewed in Section II. Then, experimental results on the availability of precise GNSS measurements with various receivers and antenna locations, and their suitability for precise positioning, are presented in Section III. Finally, Section IV concludes the paper and gives an outline for future work.

II. Methods for Precise GNSS Positioning

The basic GNSS observables are the pseudorange ρ and the carrier phase ϕ; these measurements can be modeled in units

978-1-4799-8915-7/16/$31.00

of meters for satellite i as

$$\rho_i = \|\mathbf{p} - \mathbf{p}_i - \delta\mathbf{p}_i\| + c\,(\delta t - \delta t_i) + I_i + T_i + \varepsilon_i \quad (1a)$$

$$\phi_i = \|\mathbf{p} - \mathbf{p}_i - \delta\mathbf{p}_i\| + c\,(\delta t - \delta t_i) - I_i + T_i + \lambda N_i + \eta_i \quad (1b)$$

where $\mathbf{p}$ and $\mathbf{p}_i$ denote the positions of the user and the ith satellite, respectively; $\delta\mathbf{p}_i$ represents the error in the broadcast satellite position. The receiver and satellite clock biases are denoted by δt and δt_i, respectively. c is the speed of light and λ denotes the signal wavelength. Propagation delays due to the ionosphere and troposphere are represented by I_i and T_i, respectively; N_i is the carrier phase cycle ambiguity. Finally, unmodeled error sources such as measurement noise, multipath, and antenna imperfections are denoted by ε_i for the pseudorange and by η_i for the carrier phase; in general, the variance of pseudorange noise is larger than its carrier phase counterpart by several orders of magnitude.

Obviously, the key to high-precision GNSS positioning is a careful compensation of the error terms involved in the measurement models (1). In the following sections, two different precise positioning approaches are presented: Real-Time Kinematic (RTK) positioning which utilizes raw measurements from a base station and Precise Point Positioning (PPP) that uses external assistance data to mitigate the errors of a standalone receiver.

A. Real-Time Kinematic Positioning

RTK is a method of differential positioning and takes advantage of the spatial and temporal correlation of ranging errors due to the space segment and the propagation medium. If a base station with a known position is available in the vicinity of the user, differencing the measurements (1) made for satellite i by the user and the base station, satellite and atmosphere related errors are entirely canceled out or at least significantly mitigated. Furthermore, the difference of such differential measurements constructed for satellites i and j, called a double difference, cancels out errors due to the receiver clocks.

A key benefit of the double difference is that it also cancels out fractional phase biases of the receivers and the satellite, which implies that the double differenced carrier cycle ambiguity is of integer nature. Solving for these integer ambiguities, e.g., using the LAMBDA method [2], makes it possible to estimate the baseline between the user and the base station at centimeter-level precision or even better. Unfortunately, the wavelength of GNSS signals is in the order of 0.2 meters, which makes ambiguity resolution a challenging task. Multi-frequency receivers can facilitate the problem by combining observations made at different frequencies, but currently, such receivers are beyond the price level of consumer devices. So far no single-frequency RTK solution has become popular in the mass market.

B. Precise Point Positioning

As opposed to relative RTK, the approach of PPP is absolute positioning without using base stations. PPP uses external correction data, such as precise satellite ephemerides, to eliminate the error terms from the measurements (1). The most significant factor is the ionospheric error which can be addressed in several different ways. Multi-frequency receivers can exploit the dispersivity of the ionosphere to cancel the error out; single-frequency users need to either use an external ionosphere map or utilize the fact that the sign of the ionosphere error is positive in (1a) but negative in (1b) [10]. However, the combination of the two observables is susceptible to the pseudorange noise ε.

Traditionally, PPP has been done without explicitly resolving the carrier cycle ambiguities but waiting for the ambiguities to converge without enforcing integer constraints, which can take dozens of minutes. Recently, the availability of satellite phase bias corrections has raised interest in ambiguity-fixed PPP [3], [11]. However, in this paper, no such corrections are used and, therefore, the PPP solutions are computed with floating point ambiguities; an accuracy in the order of decimeters can then be expected [12].

Although PPP avoids the burden of setting up a base station, a source of correction data is needed. For instance, the International GNSS Service (IGS) [13] provides precise satellite ephemerides, ionosphere maps, and other products free of charge. Recently, national services providing country-wide state-space representation error models [14], [15] have been developed. Although PPP has traditionally been a post-processing technique, it is today feasible in real time as the correction data can be streamed, e.g., using the NTRIP protocol.

PPP has two important benefits over RTK. First, the correction data do not change rapidly, which can lead to communication bandwidth savings in comparison with broadcasting raw base station measurements for every epoch. Second, the PPP correction data are usually valid for a large area, e.g., a country or even the entire globe; therefore, the user has no need to disclose his or her exact position to the correction data service, which improves user privacy.

III. Experimental Results

Two field tests were done on October 22, 2015, to collect GNSS data with various receivers for the analysis. The first test was carried out in the morning in the suburbs of London, United Kingdom, starting at Heathrow Airport and driving along motorway M4 towards the city for approximately 27 minutes. The second experiment was done downtown London in the afternoon and yielded 13 minutes worth data.

In the following sections, we first describe the instrumentation used in the experiments. Then, the availability of carrier phase measurements and the received signal strength distributions for both test environments are analyzed. Finally, PPP solutions are computed and the accuracy attained with different receivers and installation points is discussed.

A. Test Setup

In order to investigate the availability of precise carrier phase measurements in ITS scenarios, a total of five GNSS

Fig. 1. The test vehicle

receivers were installed on the test vehicle which was a van provided by Transport for London (see Fig. 1). One of the receivers was integrated with a tactical grade INS [16] with the antenna mounted on the roof of the test vehicle. Together with RTK reference station data, the measurements made by this system were post-processed using Waypoint Inertial Explorer to obtain a reference position solution.

The remaining four receivers were set up as follows. A Leica Viva GS15 GNSS receiver was installed on the roof of the test van along with the reference receiver's antenna and an active patch antenna that was connected to a low-cost U-Blox NEO-7P GPS receiver; see Fig. 2a[1]. Inside the cabin, an identical U-Blox receiver with patch antenna and a Nokia Lumia 1520 smartphone running a tailored firmware were set up on the dashboard as shown in Fig. 2b. This special phone, courtesy of Microsoft Mobile, allows access to the raw pseudorange and carrier phase measurements made by its internal GNSS receiver. The devices were mounted on the dashboard in order to have satellite signal reception conditions similar to a portable device that needs to be in the driver's view.

Position solutions were computed using RTKLIB [17] in the 'Kinematic PPP' mode; the base stations were located more than 5 kilometers away from the test routes, making it difficult to obtain ambiguity-fixed single-frequency RTK solutions. Final satellite orbit and clock products by the European Space Operation Center [18] and final ionosphere maps by the IGS were used as the external correction data while the Saastamoinen model was used to mitigate the tropospheric delay. Furthermore, position offsets due to solid Earth tides were compensated for using the spherical harmonics model [19]. A cutoff elevation of 15° was chosen to ignore the most error-prone signals, but no other a priori exclusions, such as carrier-to-noise-density ratio (C/N_0) thresholds, were employed.

The analysis in the following sections focuses on the

[1]In addition to the GNSS antennas, there were other antennas mounted on the roof of the vehicle. Their possible mutual interference has not been investigated.

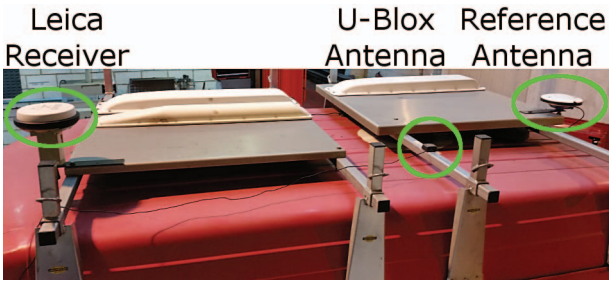

(a) Roof; also note the presence of flat white iBus antennas (not part of the experiment)

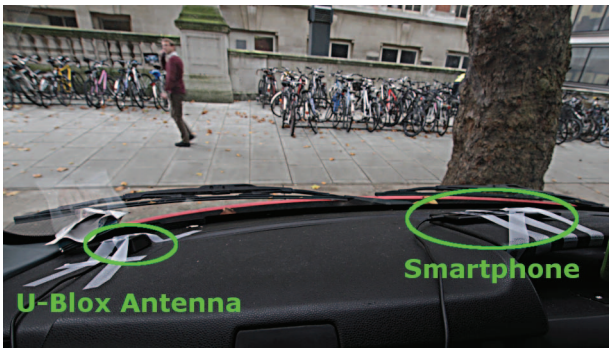

(b) Dashboard

Fig. 2. Locations of the receivers and the antennas on the test vehicle

smartphone and the U-Blox receivers. Since the smartphone supports both GPS and GLONASS, its measurements were processed in both GPS-only and GPS+GLONASS configurations in order to establish a fair comparison with the GPS-only U-Bloxes. The purpose of the Leica receiver was to only verify that the performance of the PPP processing software and the quality of the correction data are sufficient for the accuracy analysis; it is not included in the measurement availability investigation. Unfortunately, the U-Blox with antenna on the roof was unavailable during the second experiment because of technical problems.

B. Measurement Availability

To assess the availability of good quality carrier phase measurements, we study the raw measurement data from the different receivers from two perspectives. First, we construct histograms of the C/N_0 distributions for *all* satellites tracked by each receiver in order to get a grasp on the signal power lost inside the vehicle. Then, we count the number of *usable* carrier phase measurements for each epoch in order to assess the feasibility of precise GNSS positioning with the received sets of observations.

The distributions of C/N_0 estimates for all GPS satellites tracked by the low-cost receivers are shown in Fig. 3; note that the histograms have been normalized by the total measurement count of each receiver. The difference between the roof-mounted and inside-cabin U-Bloxes in the suburban test is evident; the roof receiver's C/N_0 distribution has both a higher mean and a lower variance. It is also seen that these two receivers produced a significantly skewed C/N_0 distribution

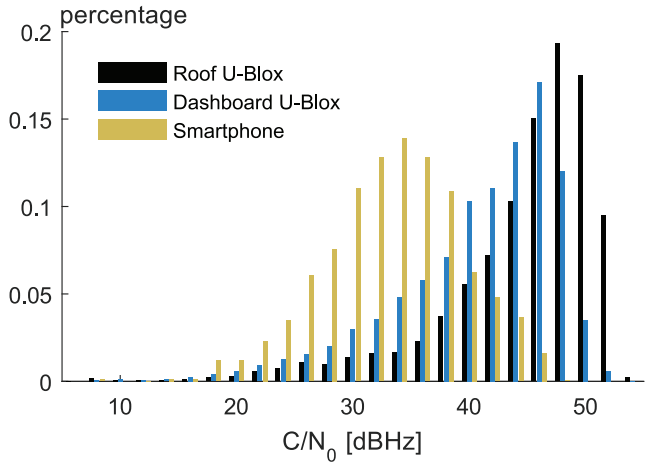

(a) Suburban Test

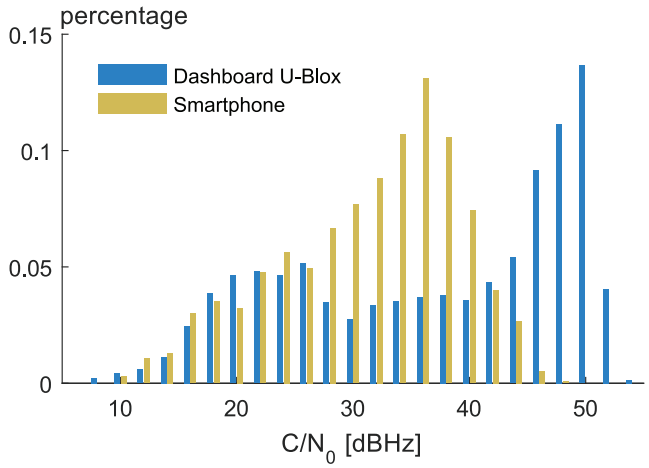

(b) Urban Test

Fig. 3. Normalized C/N_0 measurement histograms

as opposed to the smartphone whose distribution is quite symmetric. The phone's histograms include both GPS and GLONASS signals and its mean is approximately 10 dB lower than that of the dashboard-mounted U-Blox, which conforms with the observation made in [9] that the noise level is considerably higher in the smartphone's GNSS measurements than in the U-Blox. However, the histograms for the urban test show remarkably similar distributions for the dashboard U-Blox and the smartphone around the 20 dBHz region.

For estimating the amount of usable carrier phase measurements, certain criteria were chosen. First, it was required that the measurements do not have a cycle slip flag enabled by the receiver. Second, a C/N_0 threshold of 25 dBHz was chosen. The number of measurements satisfying these criteria were counted epoch-wise for each receiver; moreover, they were sorted to five C/N_0 brackets to illustrate the expected quality of the measurements. However, it should be noted that the U-Blox receivers output cycle slip flags conformant with the RINEX loss of lock indicator [20] while the smartphone does not. Therefore, it is likely that the cycle slip criterion is stricter for the U-Bloxes, but, on the other hand, their results can be seen as lower bounds.

The results for the suburban test are shown in Fig. 4. It can be seen that the roof and dashboard U-Bloxes receive 7 or more good carrier phase signals for most of the time; in fact, this amount has been observed sufficient for reaching a sub-meter position accuracy in single-frequency PPP [12]. The roof-mounted receiver has a somewhat larger number of good signals, and it is also seen that the proportion of signals with $C/N_0 \geq 45$ dBHz is significantly higher. Nevertheless, most of the good signals exceed 35 dBHz for the dashboard U-Blox as well. In contrast, the smartphone received up to three GPS signals with $C/N_0 \geq 35$ dBHz for most of the epochs; it can be seen that the inclusion of GLONASS improves the situation slightly, but the amount of very strong signals remains negligible, as predicted by the histograms in Fig. 3.

As can be expected, the amount of received signals decreases when moving to an urban environment. The signal counts for the urban test are shown in Fig. 5. Note that since the roof U-Blox was unavailable in this test, Fig. 5a shows the number of signals satisfying both criteria for a good signal for the dashboard U-Blox, analogously to Fig. 4b, while Fig. 5b shows the signal counts without the cycle slip flag constraints, depicting values better comparable with the smartphone measurements in Fig. 5c and 5d. It can be seen that there are only a handful of epochs where the number of measurements passing the cycle slip criterion exceeded 6 for the dashboard U-Blox; relaxing that criterion gives 7 signals with $C/N_0 \geq 30$ dBHz available for most of the time. However, with the smartphone the situation is even more challenging: with GPS only, there are few epochs with 7 or more satellites with $C/N_0 \geq 30$ dBHz; again, having GLONASS helps, but is not enough to keep the number of strong signals steadily close to 7.

C. Positioning Accuracy

Since the horizontal position is of prime importance in ITS, we will evaluate the positioning accuracy distributions in terms of circular error probables (CEP). The CEP for a certain probability is defined as the radius of the disk on the horizontal plane centered at the reference location (obtained from Inertial Explorer) that contains the estimated position for the given percentage of solution epochs. In this article, epochs with no valid position solution are *not* excluded from the computation of CEPs; in other words, if the position availability for a certain data set is, e.g., 94 %, then no CEP95% exists for that set. The position is defined to be *available* for a certain epoch if RTKLIB outputs a position solution for it (regardless of the accuracy).

Horizontal positioning results for the suburban test are shown in Table I. It can be seen that all receivers and configurations delivered an availability better than 90 %; it should be noted that the test route visited Heathrow Tunnel Road E approx. 3 minutes after the beginning of the test, causing a notable GNSS unavailability period. The U-Bloxes performed better than the smartphone, as can be expected based on the measurement availability analysis made in the

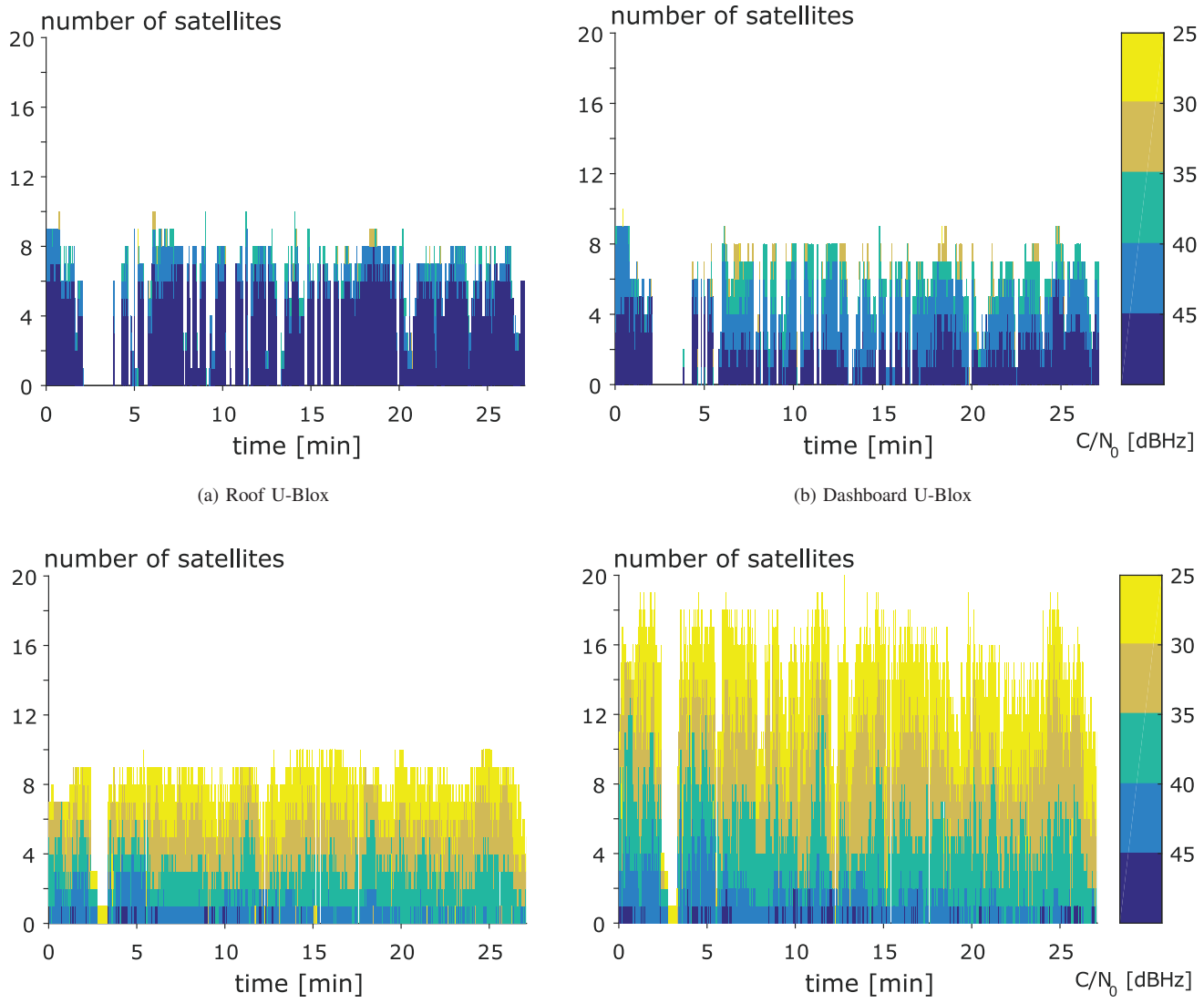

(a) Roof U-Blox

(b) Dashboard U-Blox

(c) Smartphone; GPS satellites only

(d) Smartphone; GPS and GLONASS satellites

Fig. 4. Number of usable satellites with carrier phase measurements in the suburban test

TABLE I
HORIZONTAL PPP ACCURACY AND AVAILABILITY (AVL) IN THE SUBURBAN TEST

Receiver	Circular Error Probable [m]				Avl [%]
	50 %	70 %	90 %	95 %	
Roof U-Blox	1.05	1.38	2.30	4.45	97.4
Dashboard U-Blox	1.71	2.63	4.70	9.40	96.9
Smartphone, GPS only	6.32	9.13	18.92	–	94.6
Smartphone, GPS+GLO	6.22	8.13	14.28	28.54	96.7
Leica	0.66	0.76	1.24	–	94.0

previous section; therefore, the discrepancy is not expected to be resolvable by tuning the positioning filter parameters. Furthermore, the dashboard U-Blox seems to have the CEPs approximately twice as large as those for its roof-mounted counterpart; in fact, a similar relationship seems to hold for the roof-mounted U-Blox and the professional grade Leica. Although the achieved accuracy figures exceed one meter (except for the Leica), it should be kept in mind that they were obtained using unaided GNSS; assistance information, e.g., map matching, could improve the accuracy further.

Table II shows the positioning accuracy in the urban test. It is not surprising that the results are degraded in comparison to the suburban test; even the professional grade Leica is far from lane-level accuracy in the single-frequency CEP70% and has a GNSS position solution available for less than 75 % of the time. In contrast, the U-Blox delivers a surprisingly high availability of 99.9 % on the dashboard even though it seems to have less than four satellites available for several minutes in Fig. 5b; an explanation could be that RTKLIB has been using satellites for which a valid carrier phase has not been

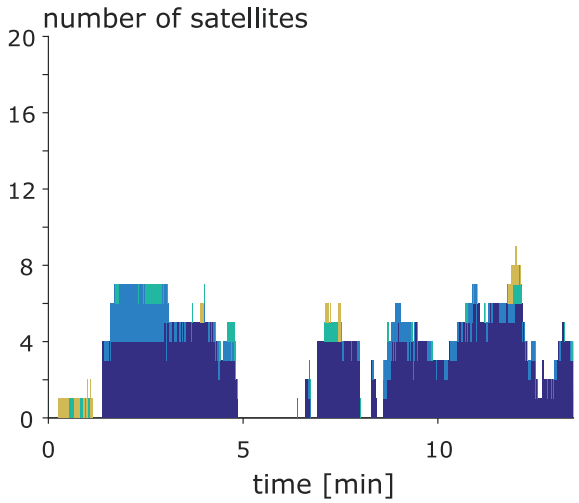

(a) Dashboard U-Blox; cycle slip free signals only

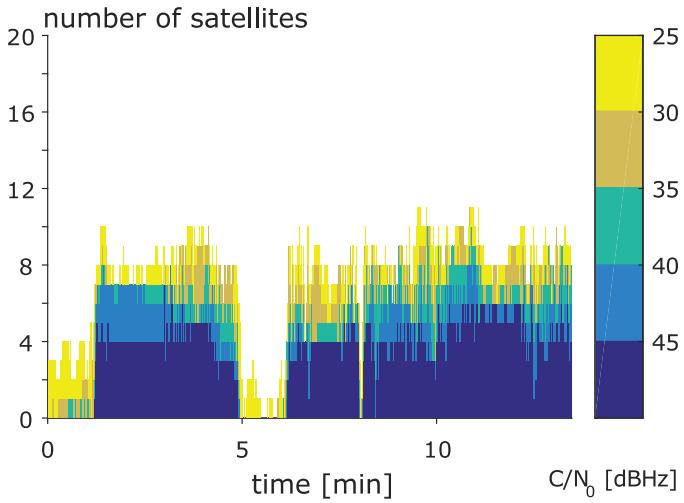

(b) Dashboard U-Blox; no cycle slip flag constraints

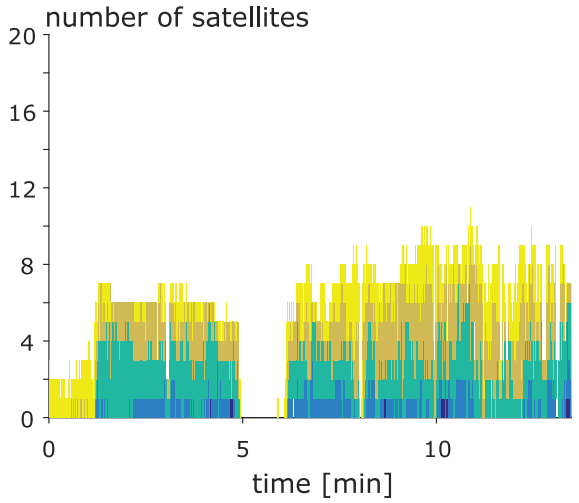

(c) Smartphone; GPS satellites only

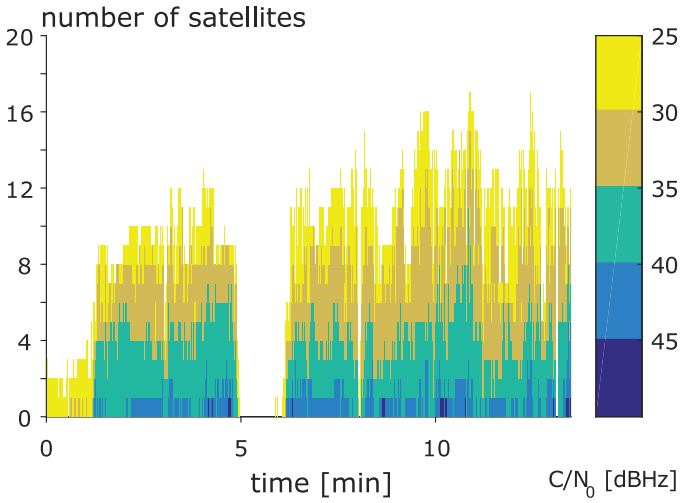

(d) Smartphone; GPS and GLONASS satellites

Fig. 5. Number of usable satellites with carrier phase measurements in the urban test

available. Nevertheless, it is seen that the U-Blox with antenna next to the smartphone yields approx. 50 % more accurate positioning results; when using GLONASS in addition to GPS, the smartphone gets relatively close to the accuracy of the GPS-only U-Blox in CEP70% and CEP90%, though.

As the reference receiver was integrated with an INS, a precise heading estimate is available for each epoch. Using this information and the measured offsets of the other antennas with respect to the reference, the reference position of each antenna could be computed separately. The lever arm measurements are accurate to the centimeter level for the roof-mounted antennas and to the decimeter level for the receivers inside the cabin. Furthermore, the estimated three-dimensional error standard deviation for the reference solution computed by Inertial Explorer never exceeded 0.5 meters in either test, with the median 3D standard deviation being less than 0.1 m. Therefore, inaccuracies in the reference RTK solution are expected to be dominated by the errors in the single-frequency PPP solutions.

TABLE II
HORIZONTAL PPP ACCURACY AND AVAILABILITY (AVL) IN THE URBAN TEST

Receiver	Circular Error Probable [m]			Avl [%]
	50 %	70 %	90 %	
Dashboard U-Blox	6.22	19.77	41.24	99.9
Smartphone, GPS only	17.36	28.78	107.12	92.3
Smartphone, GPS+GLO	13.45	22.16	53.94	94.3
Leica	1.39	11.07	–	74.7

IV. Conclusions and Future Work

This paper investigated the effect of antenna location for precise low-cost GNSS positioning for a land vehicle. The expected loss in positioning performance for the receivers located inside the vehicle cabin was clear both in the received C/N_0 distributions and the resulting position CEPs. Moreover, it was seen that the GNSS positioning accuracy of the smartphone is not comparable with an adjacent low-cost GNSS receiver using an active patch antenna inside the cabin of the vehicle; most likely the difference is due to many factors, e.g., different tracking sensitivities in addition to the antenna quality. Therefore, additional challenges need to be addressed when implementing precise positioning on a mobile low-cost ITS terminal.

The positioning results presented in this paper were obtained using GNSS measurements only. As future work, it should be studied how the results change when all GNSS systems, including Galileo and BeiDou, are being used—it is evident that the number of good measurements would be increased. Furthermore, the accuracy could be improved by integrating precise GNSS positioning with other sources of information; for instance, road maps are likely to be available in ITS applications, and access to on-board sensor data such as speed measurements would further enhance the performance. Such assistance is crucial in urban environments where already the CEP70% values were observed to exceed 10 meters, even with the professional grade receiver.

Acknowledgment

This article is based upon work from COST Action TU1302 "Satellite Positioning Performance Assessment for Road Transport" (SaPPART), supported by COST (European Co-operation in Science and Technology).

Furthermore, this research was supported by the National Natural Science Foundation of China (61328301, 61401435 and 61403253) and the project P3-Service (Public Precise Positioning) funded by Destia Oy, Fastroi Oy, Hohto Labs Oy, Indagon Oy, TeliaSonera Finland Oyj, Microsoft Mobile, Space Systems Finland Oy, Semel Oy, VR Track Oy, the Finnish Technology Agency TEKES, and the Finnish Geospatial Research Institute.

The authors would also like to thank Dr Mauro Manela and Mr Mark Sapsford at Transport for London (TfL) for helping the trial carried out on 22nd of October 2015.

References

[1] F. Peyret, P.-Y. Gilliéron, L. Ruotsalainen, and J. Engdahl, "SaPPART white paper: Better use of global navigation satellite systems for safer and greener transport," French Institute of Science and Technology for Transport, Development and Networks (Ifsttar), Les collections de l'Ifsttar – techniques et méthodes – TMI 1, Sep. 2015.

[2] P. J. G. Teunissen, P. J. de Jonge, and C. C. J. M. Tiberius, "The LAMBDA-method for fast GPS surveying," in *Proc. International Symposium "GPS Technology Applications"*, Bucharest, Romania, Sep. 1995.

[3] A. Jokinen, S. Feng, W. Schuster, W. Ochieng, C. Hide, T. Moore, and C. Hill, "GLONASS aided GPS ambiguity fixed precise point positioning," *Journal of Navigation*, vol. 66, no. 3, pp. 399–416, May 2013.

[4] S. Söderholm, "GPS L1 carrier phase double difference solution using low cost receivers," in *Proc. ION GNSS*, Long Beach, CA, Sep. 2005, pp. 376–380.

[5] J. Engelbrecht, M. J. Booysen, G.-J. van Rooyen, and F. J. Bruwer, "Survey of smartphone-based sensing in vehicles for intelligent transportation system applications," *IET Intelligent Transport Systems*, vol. 9, no. 10, pp. 924–935, Dec. 2015.

[6] T. Menard, J. Miller, M. Nowak, and D. Norris, "Comparing the GPS capabilities of the Samsung Galaxy S, Motorola Droid X, and the Apple iPhone for vehicle tracking using FreeSim_Mobile," in *Proc. 14th International IEEE Conference on Intelligent Transportation Systems*, Oct. 2011, pp. 985–990.

[7] C. Bauer, "On the (in-)accuracy of GPS measures of smartphones: A study of running tracking applications," in *Proc. 11th International Conference on Advances in Mobile Computing & Multimedia*, Vienna, Austria, Dec. 2013, pp. 335–340.

[8] K. M. Pesyna, Jr., R. W. Heath, Jr., and T. E. Humphreys, "Centimeter positioning with a smartphone-quality GNSS antenna," in *Proc. ION GNSS+*, Tampa, FL, USA, Sep. 2014, pp. 1568–1577.

[9] M. Kirkko-Jaakkola, S. Söderholm, S. Honkala, H. Koivula, S. Nyberg, and H. Kuusniemi, "Low-cost precise positioning using a national GNSS network," in *Proc. ION GNSS+*, Tampa, FL, USA, Sep. 2015, pp. 2570–2577.

[10] T. P. Yunck, "Orbit determination," in *Global Positioning System: Theory and Applications, Volume II*, ser. Progress in Astronautics and Aeronautics, B. W. Parkinson and J. J. Spilker Jr., Eds. Washington, DC, USA: American Institute of Aeronautics and Astronautics, Inc., 1996, vol. 164, pp. 559–592.

[11] J. Geng, F. N. Teferle, X. Meng, and A. H. Dodson, "Towards PPP-RTK: Ambiguity resolution in real-time precise point positioning," *Advances in Space Research*, vol. 47, no. 10, pp. 1664–1673, May 2011.

[12] P. de Bakker and C. Tiberius, "Real-time single-frequency precise point positioning on the road, and on track," in *Proc. ION GNSS+*, Tampa, FL, USA, Sep. 2015, pp. 1096–1114.

[13] J. M. Dow, R. E. Neilan, and C. Rizos, "The International GNSS Service in a changing landscape of Global Navigation Satellite Systems," *Journal of Geodesy*, vol. 83, no. 3, pp. 191–198, Mar. 2009.

[14] M. Kirkko-Jaakkola, J. Saarimäki, S. Söderholm, R. Guinness, L. Ruotsalainen, H. Kuusniemi, H. Koivula, T. Mattila, and S. Nyberg, "P3: A public precise positioning service based on a national GNSS network," in *Proc. International Conference on Localization and GNSS*, Helsinki, Finland, Jun. 2014.

[15] M. Miya, Y. Sato, S. Fujita, N. Motooka, M. Saito, and J.-i. Takiguchi, "Centimeter level augmentation service (CLAS) in Japanese Quasi-Zenith Satellite System, its preliminary design and plan," in *Proc. ION GNSS+*, Tampa, FL, USA, Sep. 2014, pp. 645–652.

[16] *iTraceRT-F200-E*, data sheet, rev. 3.3, iMAR GmbH, St. Ingbert, Germany, Apr. 2013.

[17] T. Takasu and A. Yasuda, "Development of the low-cost RTK-GPS receiver with an open source program package RTKLIB," in *Proc. International Symposium on GPS/GNSS*, Jeju, Korea, Nov. 2009.

[18] "ESOC IGS analysis strategy," European Space Operation Center, Darmstadt, Germany, Nov. 2011, accessed 21 Jan 2016. [Online]. Available: https://igscb.jpl.nasa.gov/igscb/center/analysis/esa.acn

[19] D. D. McCarthy and G. Petit, "IERS conventions (2003)," International Earth Rotation and Reference Systems Service, Frankfurt am Main, Germany, IERS Tecnical Note 32, 2004.

[20] "RINEX: The receiver independent exchange format," International GNSS Service and RTCM Special Committee 104, Jul. 2015, version 3.03.